INSILI 1 (2025) 100042

Contents lists available at ScienceDirect

In Silico Research in Biomedicine

journal homepage: www.sciencedirect.com/journal/in-silico-research-in-biomedicine

Molecular mechanisms of sea cucumber bioactive compounds in anti-infertility treatment: *In silico* and *In vivo* approach

Irena Ujianti [a,*], Mulyoto Pangestu [b], Supandi [c], Bety Semara Lakhsmi [d], Wawang S Sukarya [e], Zahra Nurusshofa [f], Takashi Yashiro [g]

[a] *Department of Medical Physiology, Faculty of Medicine, Universitas Muhammadiyah Prof. DR. HAMKA, Jakarta, Indonesia*
[b] *Department of Obstetric Gynaecology, Faculty of Medicine, Nursing and Health Science, Monash University, Clayton, Australia*
[c] *Department of Pharmaceutical Chemistry, Faculty of Pharmacy and Science, Universitas Muhammadiyah Prof. Dr. HAMKA, Indonesia*
[d] *Department of Obstetric Gynaecology, Faculty of Medicine, Universitas Muhammadiyah Prof. DR. HAMKA, Jakarta, Indonesia*
[e] *Department of Public Health, Faculty of Medicine, Universitas Muhammadiyah Prof. DR. HAMKA, Jakarta, Indonesia*
[f] *Department of Pathology Anatomy, Faculty of Medicine, Universitas Muhammadiyah Prof. DR. HAMKA, Jakarta, Indonesia*
[g] *Jichi Medical University, School of Medicine, Japan*

A R T I C L E I N F O

Keywords:
Sea cucumber
Infertility
Network pharmacology
Bioactive compounds
Estrogen receptor
Androgen receptor
Molecular docking
Molecular dynamics
In vivo

A B S T R A C T

Background: Infertility affects 15% of couples worldwide and is often associated with oxidative stress and inflammation. Sea cucumbers, traditionally used in medicine, may offer a promising new approach to infertility treatment due to their beneficial properties, although the underlying mechanisms remain not fully understood.
Purpose: This study aimed to elucidate the molecular mechanisms underlying the anti-infertility effects of sea cucumber using a network pharmacology approach, with a focus on interactions with key hormone receptors and signaling pathways and *in vivo* study.
Study design: This experimental study employed *in silico* and *in vitro* methods to evaluate the potential of *Stichopus herrmanni* extracts in the treatment of infertility.
Methods: Bioactive compounds from sea cucumber extracts were identified via LC-MS. The potential for infertility treatment was assessed using the WAY2DRUG PASS server, while ADMET analysis determined drug-likeness. Protein targets were predicted using the SEA Search Server and Swiss Target Prediction, and cross-referenced with the DisGeNET and Open Targets databases. Network topology analysis was conducted using STRING and Cytoscape. Docking analysis and molecular dynamics simulations were performed to investigate interactions with estrogen receptor alpha (ESR1) and androgen receptor (AR). *In vivo* tests involved administering 300 mg/kg of sea cucumber extract to male rats with regular or high-fat diets for eight weeks.
Results: Twentynine bioactive compounds exhibited anti-infertility potential. Notably, andrographolide and 6-gingerol strongly bound to ESR1 and AR, with stable interactions confirmed by molecular dynamics. *In vivo*, the extract reduced oxidative stress by increased GSH, inflammation by decreased NfkB and weight gain in high-fat diet rats.
Conclusion: This study supports the anti-infertility potential of bioactive compounds derived from sea cucumber, highlighting their promising therapeutic effect on infertility through antioxidant, anti-inflammatory mechanism.

Abbreviations: ADMET, absorption, distribution, metabolism, excretion, and toxicity; AR, androgen receptor; BC, bioactive compound(s); BP, biological process; cAMP, cyclic adenosine monophosphate; CID, compound identifier; CPI, compound-protein interactions; CYP17A1, cytochrome P450 family 17 subfamily A member 1; CYP19A1, cytochrome P450 family 19 subfamily A member 1 (Aromatase); DAVID, Database for annotation, visualization, and integrated discovery; ERα, estrogen receptor alpha; ERE, estrogen response element; ESR1, estrogen receptor1; FDR, false discovery rate; GO, gene ontology; IVF, *in vitro* fertilization; KEGG, Kyoto encyclopedia of genes and genomes; LCMS, liquid chromatography-mass spectrometry; MAPK, mitogen-activated protein kinase; MCODE, molecular complex detection; MD, molecular dynamics; MF, molecular function; MMPBSA, molecular mechanics Poisson-Boltzmann surface area; NP, network pharmacology; PCOS, polycystic ovary syndrome; PDB, protein data bank; PI3K/Akt, phosphoinositide 3-kinase/protein kinase B; PPI, protein-protein interactions; QSAR, quantitative structure-activity relationship; RG, radius of gyration; RMSD, root mean square deviation; RMSF, root mean square fluctuation; SASA, solvent accessible surface area; SC, sea cucumber; SCE, sea cucumber extract; SERM, selective estrogen receptor modulator; SMILES, simplified molecular-input line-entry system; TSV, tab separated values.

* Corresponding author.
E-mail address: irenaujianti@uhamka.ac.id (I. Ujianti).

https://doi.org/10.1016/j.insi.2025.100042
Received 26 June 2025; Received in revised form 19 July 2025; Accepted 31 July 2025
Available online 10 August 2025

Specifically, Andrographolide and 6-gingerol show promise as natural modulators of estrogen signaling. offering potential for improved reproductive health outcomes.

Introduction

Infertility is a global reproductive health issue affecting approximately 15% of couples during their reproductive years, with rates varying by region [1]. In developing countries, infertility rates can reach up to 30% in certain populations, while developed countries typically see rates between 8% and 12% [2]. The primary causes of infertility include ovulation disorders (35%), fallopian tube problems (30%), male factors (30%), and unexplained causes (5%) [3]. Female infertility involves several complex mechanisms. Polycystic ovary syndrome (PCOS), for instance, disrupts normal ovulation by causing increased androgen production and insulin resistance [4]. Other common causes include damaged fallopian tubes from infections or endometriosis, which prevent sperm from reaching the egg, and structural problems in the uterus that make it difficult for embryos to implant successfully [5]. Treatment for female infertility primarily involves regulating hormones through medications that stimulate ovulation and prepare the uterus for pregnancy. A crucial medication in this process is estradiol, which helps women with low estrogen levels by promoting the growth and development of the uterine lining [6].

Marine environments contain a wealth of natural compounds that offer safe, cost-effective, and readily available treatment options with minimal side effects [7,8]. Sea cucumbers are among these valuable marine resources, having been used in traditional medicine for centuries. Modern research now provides scientific evidence supporting their therapeutic benefits, particularly in treating infertility. Recent studies have demonstrated the significant potential of sea cucumbers as anti-infertility agents. Sea cucumber extract possesses antioxidant and anti-inflammatory properties, specifically noting their positive impact on reproductive health and fertility management [9].

A comprehensive review detailed the nutritional composition and health benefits of sea cucumbers, including specific effects on female fertility [10]. A study by Luo et al,. demonstrated the beneficial effects of sea cucumber peptide on sex hormone regulation in both normal and Premature Ovarian Failure female mice [11]. Additional laboratory research examined the cytoprotective effects of sea cucumber extracts on cryopreserved bovine sperm [12]. Supporting these findings, Moghadam demonstrated that sea cucumber saponin extract exhibits dual effects on mouse oocyte maturation through reduced oxidative stress and TNF-α expression [13]. A comperhensive review indicate that sea cucumbers show significant potential as anti-infertility agents through their antioxidant properties and positive effects on reproductive health in both men and women.

While sea cucumber extract shows promise in treating infertility, significant knowledge gaps remain regarding its specific molecular mechanisms, particularly in terms of hormonal regulation. Further research is required to clarify how these extracts influence reproductive hormone secretion, identify the cellular signalling pathways involved, and understand their interactions with hormone receptors. This study employs pharmacological network analysis to elucidate the synergistic effects and underlying mechanisms of various compounds, facilitating the evaluation of their multilevel interactions [7]. It is hoped that identifying specific bioactive compounds from sea cucumbers involved in fertility mechanisms will enable the determination of therapeutic targets and signalling pathways most relevant to understanding the potential mechanism of sea cucumbers as an anti-infertility agent in this context.

Materials and methods

Datamining and activity prediction of bioactive compounds

The bioactive compounds used in this research were derived from LCMS results of sea cucumber, as a marine organism. Subsequently, the PubChem database was used to obtain SMILES for each bioactive compound identified in the sample extract. The WAY2DRUG PASS prediction toolwas employed to assess the potential of these compounds as infertility treatments, based on their Pa Value (Probability to Be Active). The Pa value is used in the data mining process as it represents the likelihood of a compound's activity.

ADMET analysis

Sea cucumber compounds that passed activity screening based on QSAR analysis were subsequently analyzed for their pharmacokinetic characteristics. Drug-likeness was assessed for each ligand based on Lipinski's Rule of Five [14,15], using the ADMETLab 2.0 database. The input for both databases consisted of the SMILES notation for each ligand.

Protein target and gene-disease associations prediction

Protein targets were analyzed using the SEA Search Server and the Swiss Target Prediction tool [16,17]. The SEA Search Server identified protein-ligand interactions, while Swiss Target Prediction provided probabilistic associations of bioactive compounds with protein targets. Infertility-related proteins and genes were obtained from the DisGeNET database and supplemented with data from Open Targets [18,19]. Data from these sources were cross-referenced to identify proteins linked directly to infertility. This integrative approach aimed to highlight potential protein targets for use in subsequent therapeutic studies.

Graph topological network and functional annotation analysis

The compiled target protein lists from both databases were then input into the multiple protein menu of the STRING database [20]. Additional settings included selecting the organism type as *Homo sapiens*, setting the meaning of network edges and adjusting the minimum required interaction score to 0.400 (medium confidence). After updating the network based on these settings, the visualization results were downloaded in TSV (tab-separated values) format from the table/export menu. The downloaded file was then imported into Cytoscape v.3.9.0 software for subsequent network analysis through the tools menu. The Database for Annotation, Visualization, and Integrated Discovery (DAVID) was used to determine the function of genes identified in the clustering results [21].

Docking analysis

The 3D structures of target proteins ESR1 (PDB ID: 3UUD) and AR (PDB ID: 2AM9) were obtained from the PDB database, while the 3D structures of the active compounds and native ligand controls, namely estradiol (CID: 5757) and testosterone (CID: 6013), were retrieved from the PubChem database. The proteins were then prepared by removing water molecules and ligands using Discovery Studio 2021 software, and energy minimization was performed on the ligands using PyRx v.1.1 software. Docking was carried out using AutoDock Vina integrated into PyRx v.1.1. The docking procedure employed a targeted docking method with a specific gridbox. The gridbox size was adjusted according

to the position of amino acid residues based on the control ligand from the PDB and prediction results using PrankWeb [22]. The docking results were presented in terms of binding affinity, followed by RMSD calculations using DockRMSD [23]. Finally, the interactions between the compounds and proteins from the docking results were visualized using BioVia Discovery Studio 2021 software.

Molecular dynamics

This study examined four molecular systems: the estrogen receptor alpha (ESR1/ERα) alone and in complex with three different ligands—estradiol (ESR1_ETD), 6-gingerol (ESR1_6GR), and andrographolide (ESR1_ADP). Simulations were run in YASARA Dynamic with temperature set to 310K and pH to 7.4. The md_run macro set the simulation time to 20 ns using the AMBER14 forcefield, with snapshots saved every 25 ps. Analysis of potential energy, SASA, hydrogen bonds, RMSD, and radius of gyration was done with macro md_analyze. RMSF was analyzed with md_analyzeres and MMPBSA with md_analyzebindenergy. The simulation parameters were set to physiological conditions, with a temperature of 310K and a pH of 7.4.

Based on the optimal stability and binding results observed at 10 ns, molecular dynamics simulations for the specified sample and control were extended to 100 ns to further evaluate long-term behavior and binding stability. Simulations were conducted on a DELL Optiplex 7000 Tower with an i9-12900K CPU, 64GB RAM, and an Nvidia RTX 3070. The ESR1 structure was refined using Modeller10.4 via Chimera1.19. Protein and ligand preparation was performed with GROMACS 2024.5, using pdb2gmx and the charmm36-jul2021 force field for protein topology [24]. Ligand topology was generated with Avogadro, charmm36-jul2022, and CGenFF. The protein and ligand topologies were then combined, followed by solvation, addition of ions to achieve a 0.15 M concentration, equilibration, minimization, and a 100 ns molecular dynamics run at 310.15 K.

In vivo method

Stichopus hermanii extraction

Stichopus hermanii was identified from a specimen collected during a daytime dive in Lambata, East Nusa Tenggara, Indonesia, in June 2023. The sea cucumber species used in this study was confirmed as Stichopus herrmanni by a certified taxonomist, with reference number B.09.037/MSG-PD/VII/2023. The specimen was obtained from a shallow coastal habitat. To produce the sea cucumber extract, the body wall was removed and cut into small pieces approximately 1 cm in size before drying. The dried material was then mixed with ethanol in a 1:5 ratio to break down cellular proteins and extract secondary metabolites. The mixture was concentrated using a rotary evaporator set at 40°C. The final extract was prepared for use, at a dosage of 300 mg per kilogram of body weight.

Animal model

Ten-week-old healthy male Sprague Dawley rats were obtained from Institut Pertanian Bogor (IPB). The animals underwent a one-week acclimatization period in the Central Animal Lab at the Department of Chemistry, University of Indonesia, where environmental conditions were maintained at 24°C with 50% humidity. After acclimatization, the rats were randomly divided into five experimental groups of 3 rats each: control diet group with normal diet, high-fat diet group, high-fat diet plus extract group. The rats were housed individually throughout the study period, with environmental conditions maintained between 18-26°C and 50% humidity. They were fed twice daily and had free access to water, which was replaced every two days. The researchers monitored each rat's weight and size measurements monthly. Aorta homogenats tests measuring GSH and NF-κB levels were performed at the study's conclusion. The research protocol was approved by the ethics committee of Universitas Muhammadiyah Prof.Dr.HAMKA under ethical number KEPKK/FK/058/05/2024.

Table 1
Data mining structure and SMILES.

No	ESI Mode	Group	Compound Name	CID
1	(+)	Flavonoid	Nobiletin	72344
2	(+)	Terpenoid	24-Methylcholesta-7,22-dien-3β-ol	54239392
3	(+)	Terpenoid	24-Methylenecycloartanone	634880
4	(+)	Terpenoid	26-Deoxyactein	10974362
5	(+)	Terpenoid	2-Hydroxyesculentic acid	9898760
6	(+)	Terpenoid	Fibraurin	168338
7	(+)	Terpenoid	Olibanumols I	Yoshikawa, 2019
8	(+)	Terpenoid	Platycodigenin	12314399
9	(+)	Terpenoid	Scuterivulactone C2	13890624
10	(+)	Terpenoid	Stigmasta-4,22-dien-3-one	6442194
11	(+)	Terpenoid	Yesanchinoside B	1.63E+08
12	(+)	Terpenoid	Yesanchinoside H	1.63E+08
13	(-)	Phenol	6-Gingerol	442793
14	(-)	Phenol	Kukoamine A	5318865
15	(-)	Phenol	Mulberrofuran D	5467256
16	(-)	Terpenoid	3-O-(2′E,4′Z-Decadienoyl)ingenol	44575953
17	(-)	Terpenoid	Andropanolide	7067324
18	(-)	Terpenoid	Ganoderic acid H	73657194
19	(-)	Terpenoid	Hederagenin 3-O-α-L-rhamnopyranosyl-(1->2)-[β-D-glucopyranosyl(1->4)]-α-L-arabinopyranoside	73042413
20	(-)	Terpenoid	Isodihydrofutoquinol B	44715837
21	(-)	Terpenoid	Nigakilactone J	182145
22	(-)	Terpenoid	Ostruthin	5281420
23	(-)	Terpenoid	Sarcostin	46173994
24	(-)	Terpenoid	β-Cryptoxanthin palmitate	86291095
25	(+)	Terpenoid	12-Hydroxyhydromethyl	54226139
26	(+)	Terpenoid	Curculigo saponin A	85144169
27	(+)	Terpenoid	11-O-p-Coumarylnepeticin	54678486
28	(+)	Terpenoid	Curculigo saponin L	198016
29	(-)	Phenol	Nobilin C	11953937

Laboratory rat feed was sourced from Biorat Laboratory Animal Co., Ltd., including both standard and specialized high-fat, high-salt diets. The standard feed contained 10% fat, 22% protein, 68% carbohydrates, and 0.5% salt. The specialized high-fat diet had substantially higher levels of fat and salt, containing 49% fat, 21% protein, 30% carbohydrates, and 2% salt. Rats in HFD and HFD-extract groups were fed the high-fat diet and for HFD extract group received daily extract supplements of 300 mg per kilogram of body weight via gastric administration.

Measurement of GSH and NF-κB

Each rat's body weight, body size, and abdominal circumference were measured before and after treatment. Abdominal circumference (AC) was assessed on the largest zone of the rat abdomen using a plastic non-extensible measuring tape, and body size was defined as the length from nose to ani. Lee's obesity index was calculated using the formula: Lee's index = cube root of body weight (g)/body size (cm). After the rats were sacrificed, aorta tissues were sampled for homogenate tissue. The homogenized aorta samples were analyzed using ELISA kit, according to the manufacturer's protocols for the determination of NF-κB and GSH (MyBiosource, San Diego, USA). The aorta inflammation levels were normalized on the basis of the individual protein concentration.

Statistical analysis

Statistical results are presented as means ± standard deviations, with experimental groups containing 5 animals each. The specific number of animals used in each experiment is indicated in the corresponding figure legends. We performed a one-way ANOVA to assess differences between groups, followed by Tukey's post-hoc test for multiple comparisons. Results were considered statistically significant when $P<0.05$. All statistical analyses were conducted using SPSS version 20.0 software.

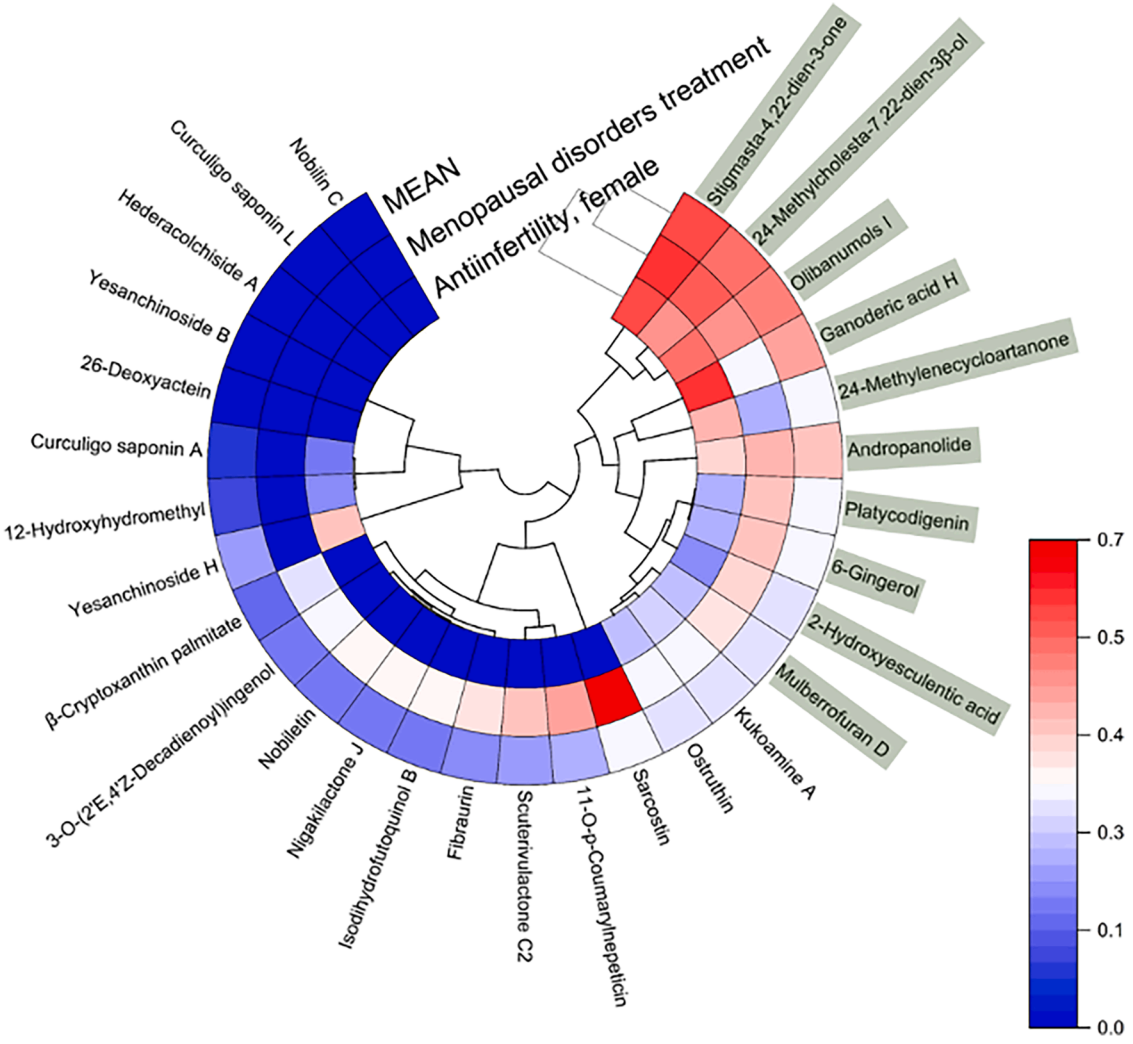

Fig. 1. Results of bioactivity potential analysis of sea cucumber compounds for anti-infertility and menopause treatment.

Table 2
Analysis results of drug-likeness and ADMET of potential compounds using AdmetLab2.0.

No	Compound Name	Druglikeness						Toxicity			
		Lipinski	MW	nHA	nHD	LogP	TPSA	H-HT	DILI	FDAMDD	Carcinogenicity
1	Stigmasta-4,22-dien-3-one	Accepted	410.35	1	0	7.477	17.07	0.247	0.715	0.955	0.121
2	24-Methylcholesta-7,22-dien-3β-ol	Accepted	398.35	1	1	7.202	20.23	0.018	0.019	0.069	0.007
3	Olibanumols I	Accepted	414.35	2	1	4.716	37.3	0.059	0.019	0.799	0.004
4	Ganoderic acid H	Accepted	572.3	9	2	2.657	152.11	0.129	0.596	0.173	0.019
5	Andropanolide	Accepted	350.21	5	3	1.754	86.99	0.023	0.058	0.966	0.032
6	Sarcostin	Accepted	382.24	6	6	0.74	121.38	0.464	0.015	0.968	0.889
7	24-Methylenecycloartanone	Accepted	438.39	1	0	7.031	17.07	0.277	0.037	0.583	0.079
8	Platycodigenin	Rejected	520.34	7	6	2.764	138.45	0.288	0.018	0.987	0.48
9	6-Gingerol	Accepted	294.18	4	2	2.765	66.76	0.224	0.042	0.847	0.082
10	Mulberrofuran D	Accepted	446.25	4	3	7.986	73.83	0.953	0.271	0.889	0.041

Results and discussion

The bioactive compounds used in this research were derived from LCMS results of the sea cucumber. Based on a search using PubChem, only 29 out of 33 identified compounds were found to be archived in the database (Table 1). Meanwhile, we drew the Olibanumols I compound ourselves using ChemSketch software, based on the 2D reference from Yoshikawa et al. [25].

The Probability to Be Active (Pa) score measures a compound's likelihood of producing therapeutic effects. This assessment compares the structural features of sea cucumber compounds to those of known effective treatments using the Way2Drug PASS Server platform. A Pa score above 0.3, represented by colours ranging from white to red, indicates a high potential for treating infertility and menopausal symptoms, as the compound's molecular structure closely resembles successful treatments in the reference database. The top ten most promising sea cucumber compounds, based on their average Pa scores, are highlighted in green in Fig. 1.

The analysis results showed that 9 out of the 10 most promising test compounds have good drug-likeness characteristics (Table 2).

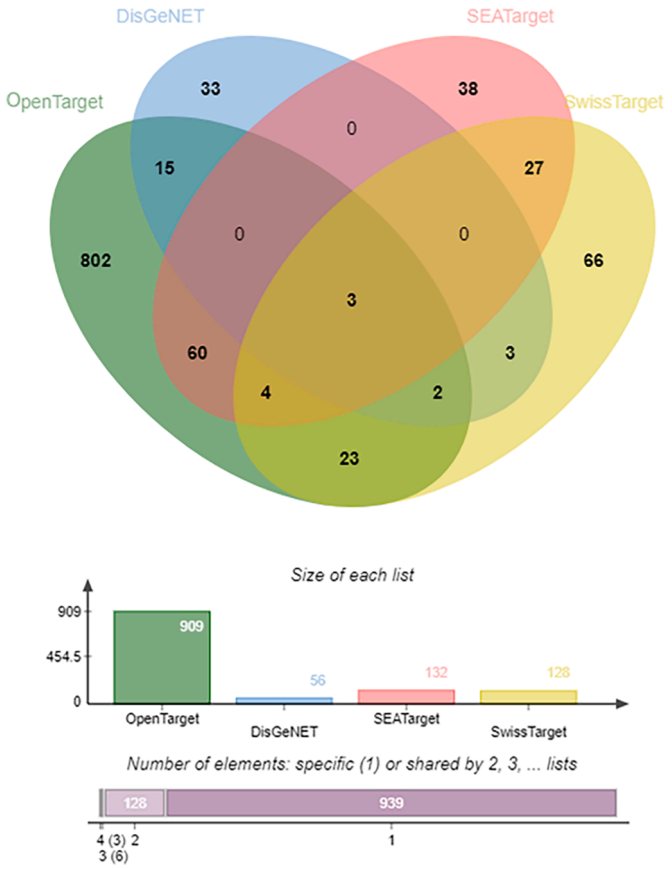

Fig. 2. Cross-target between target proteins from sea cucumber and proteins associated with anti-infertility in the database.

Platycodigenin is the only compound that does not meet Lipinski's Rule of Five for drug-likeness.

Through cross-database analysis, as illustrated in Fig. 2, we identified 12 proteins that function as potential targets for sea cucumber bioactive compounds and are linked to anti-infertility effects. Three of these proteins—CYP19A1, AR, and CYP17A1—were consistently identified across all four databases used in the study. Further analysis revealed an additional 60 proteins specific to sea cucumber compound targeting when comparing results from the SEATarget and SwissTarget databases.

Network topology analysis was conducted using Cytoscape software to examine the connections between target proteins and their interactions (PPI). The analysis focused on several key parameters: Stress, Degree, Betweenness Centrality, and Closeness Centrality. Degree centrality measures the number of connections between individual nodes, with higher values indicating proteins that interact extensively with others and may function as key regulators. Betweenness centrality evaluates the shortest path lengths used by nodes across the network, highlighting their functional importance. Closeness centrality measures how easily a node can reach others in the network, with higher values suggesting proteins that are readily accessible and potentially important regulatory hubs. In addition to these network parameters, we identified essential proteins using MCODE clustering analysis. The Molecular Complex Detection (MCODE) method is a clustering system that identifies densely interconnected regions within large protein interaction networks to detect molecular complexes. This approach is particularly effective for protein networks, as it allows for targeted cluster analysis independent of other networks and facilitates the study of cluster interconnections [26]. Our clustering analysis revealed 18 proteins forming a distinct circular cluster, separate from a second major cluster containing overlapping proteins from SEATarget and SwissTarget

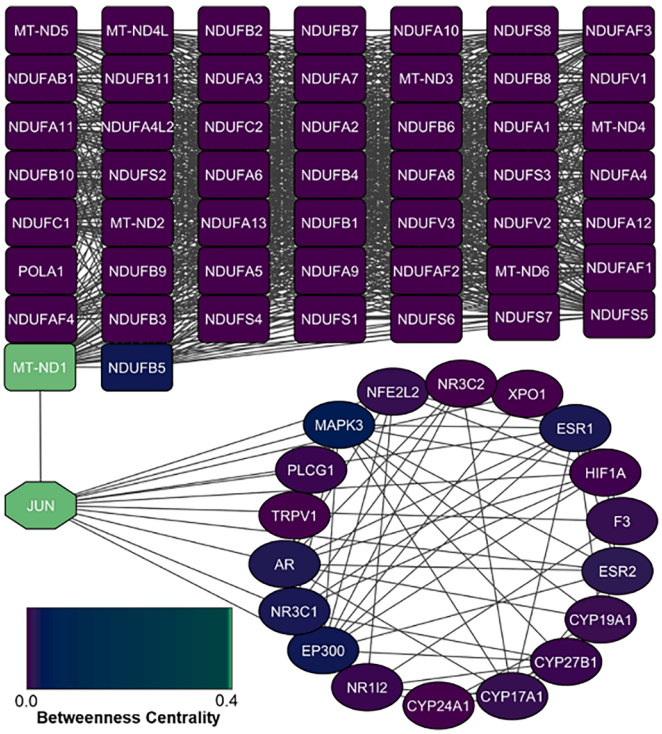

Fig. 3. Results of topological network graph analysis and MCODE clustering. Node colors approaching blue and green indicate higher dominance and increasingly important protein roles based on betweenness centrality values.

showed in Fig. 3. These 18 proteins were selected for further investigation.

Gene annotation of the 18 most potential protein/gene targets was analysed to identify their functions and roles in pathways related to infertility (Fig. 4). In addition to their relationship with infertility, the selected function and pathway annotations have a False Discovery Rate (FDR) value < 0.05. This FDR value indicates that 5% of significant tests may yield false-positive results. FDR is a statistical concept that measures the ratio of false positives to the total number of positive test results [27]. Sea cucumber extract demonstrates potential in preventing infertility in women by modulating key hormone pathways and mitigating oxidative stress. Bioactive compounds such as androponolide, sarcostin, and 6-gingerol exhibit high binding affinities to estrogen receptors (ESR1, ESR2) and androgen receptors (AR), supporting hormone regulation and signaling essential for reproductive health. Additionally, these compounds show strong antioxidative properties that protect mitochondrial function by reducing reactive oxygen species (ROS), thereby preserving oocyte quality. This dual mechanism highlights the therapeutic potential of sea cucumber extract in enhancing female fertility through hormonal balance and cellular protection.

Furthermore, based on the dominance of roles from each Biological Process (BP), Molecular Function (MF), and infertility pathways, seven of the most potential proteins/genes have been identified as target markers, namely ESR1, ESR2, AR, MAPK3, CYP17A1, CYP19A1, and NR1I2 (PRX) (Fig. 5). Proteins ESR1, ESR2, AR, MAPK3, and NR1I2 need to be activated in anti-infertility and menopause treatments [28–33]. Meanwhile, polymorphisms in CYP17A1 and CYP19A1 are associated with polycystic ovary syndrome (PCOS) and infertility [34]. Subsequently, each of the most potential target proteins as markers was mapped for their Compound-Protein Interactions (CPI) (Fig. 6).

The computational docking study revealed that, among the ten most effective compounds identified through network pharmacology, four emerged as top performers: Andropanolide, 6-Gingerol, 24-Methylcholesta-7,22-dien-3β-ol, and Sarcostin. While these compounds required higher binding energies compared to the natural PDB ligands

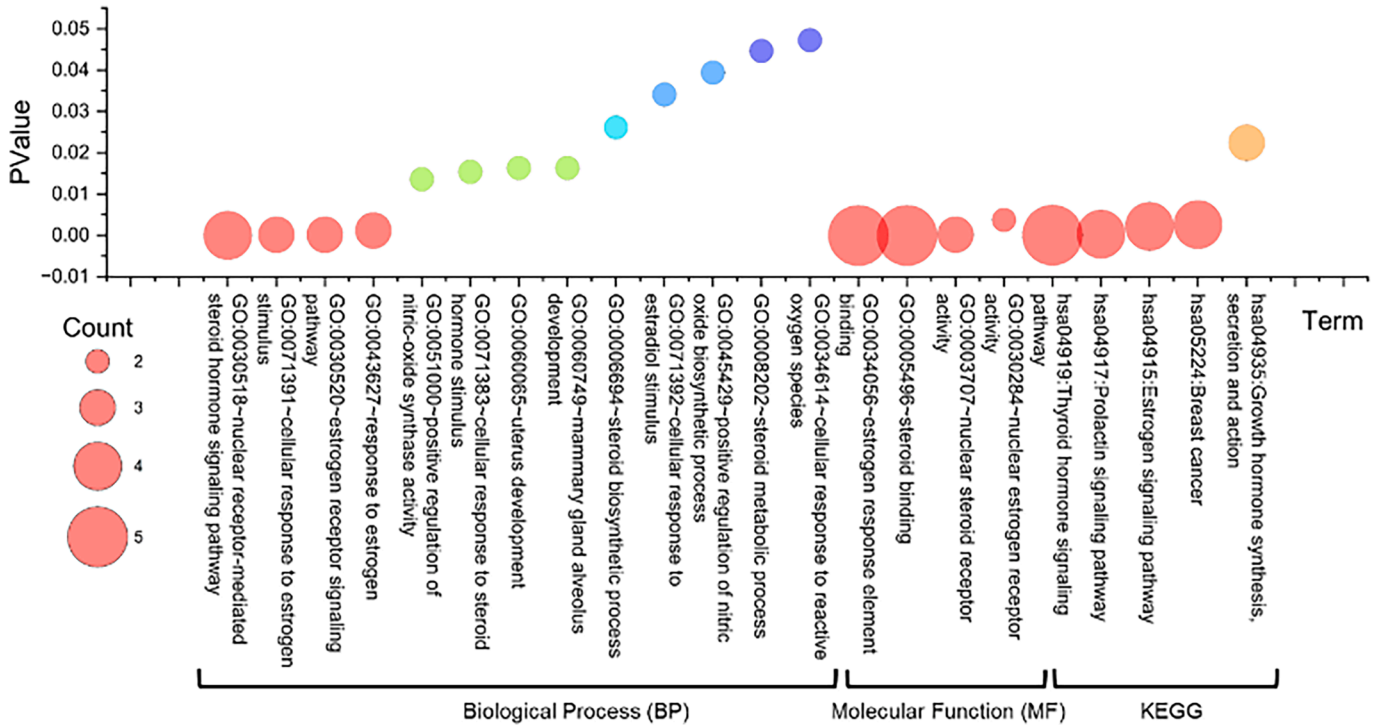

Fig. 4. GO Annotations analyzing the potential roles of sea cucumber target proteins in BP, MF and KEGG pathways related to anti-infertility treatment.

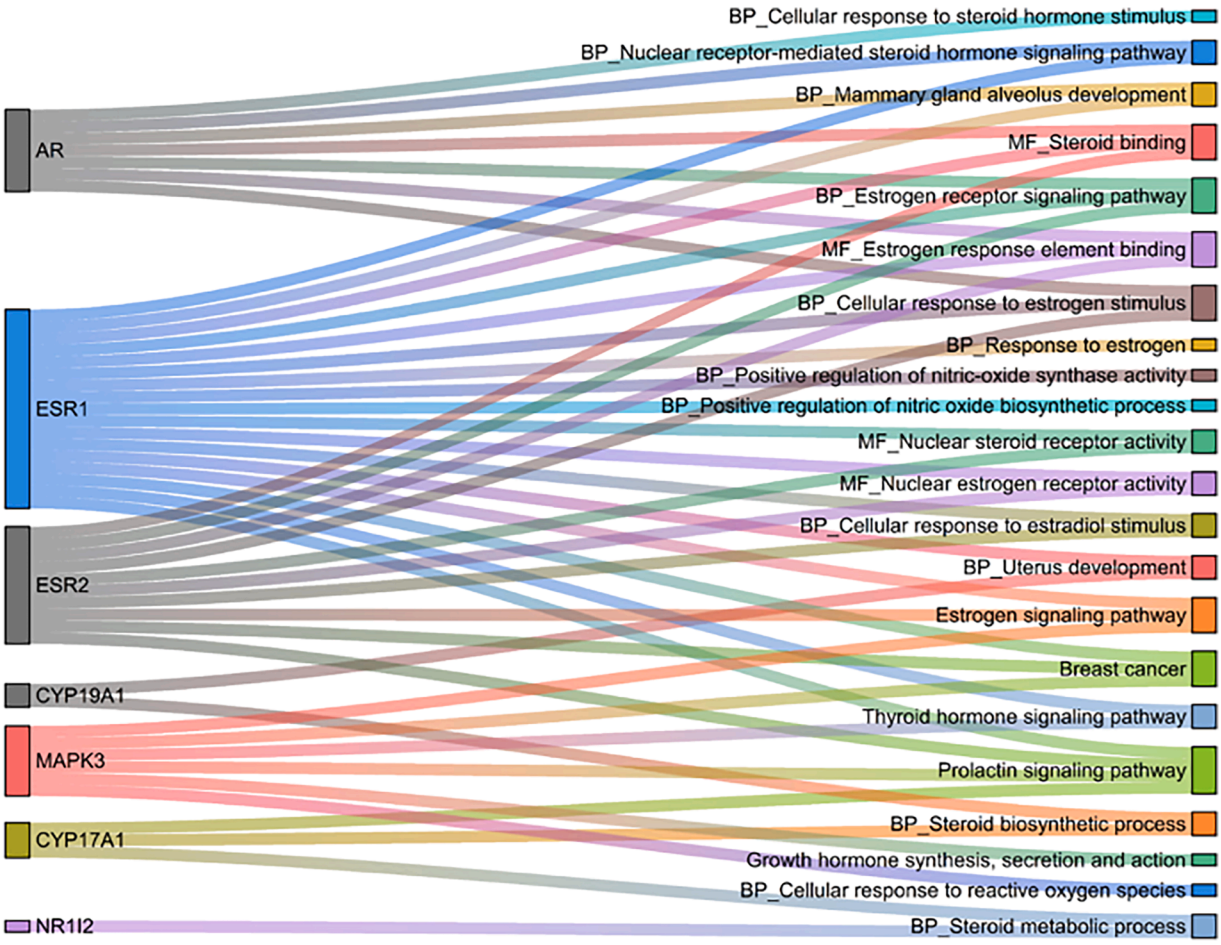

Fig. 5. Most potential proteins based on identification of potential roles.

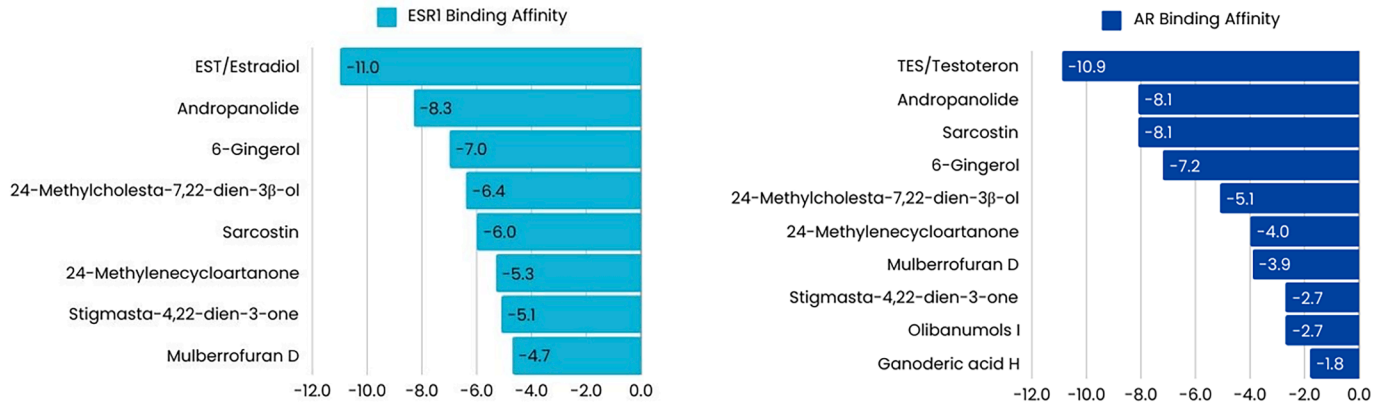

Fig. 6. the interactions formed between the target protein.

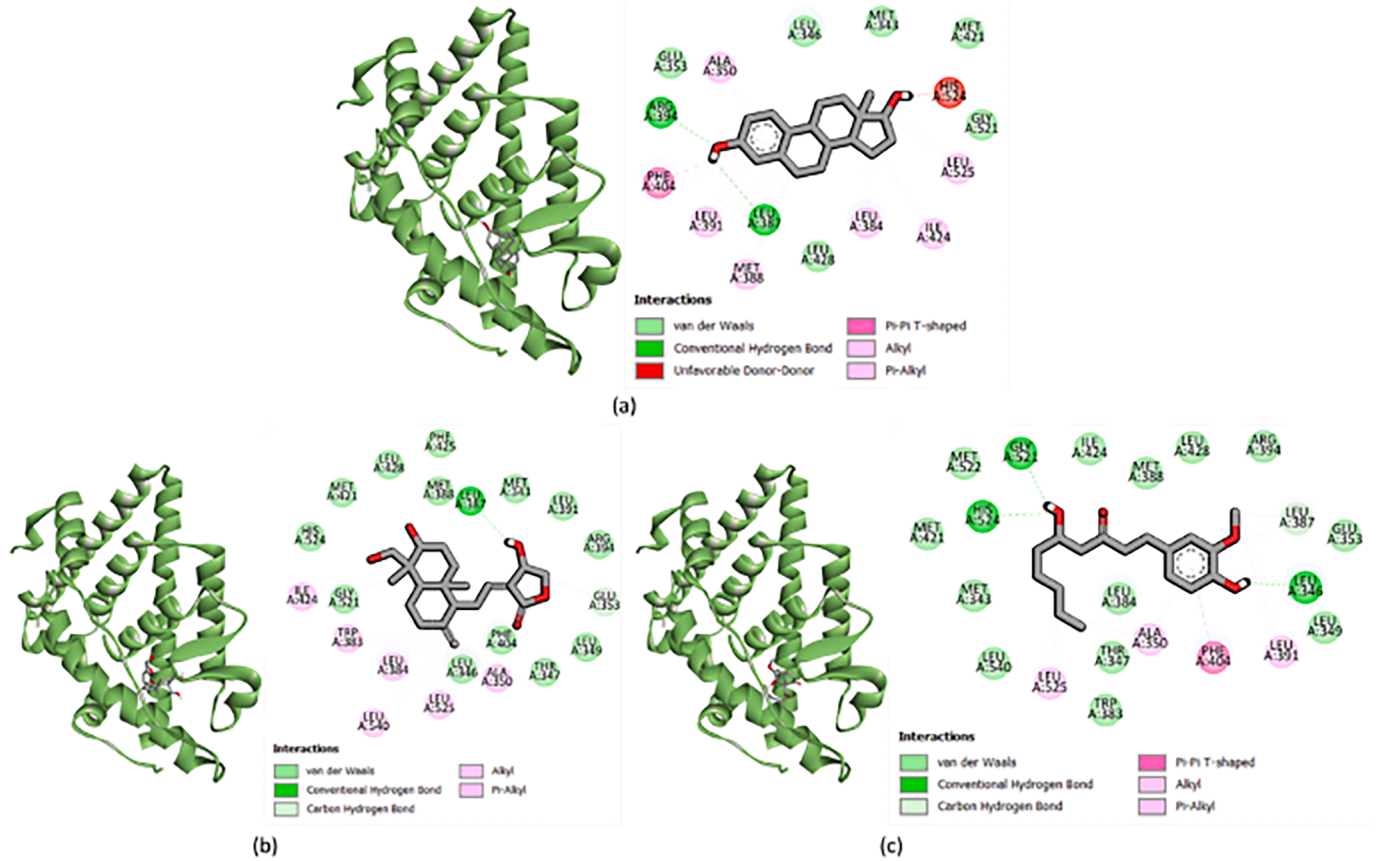

Fig. 7. Docking results visualization, a) ESR1/ER Alpha-estradiol protein (pdb control), b) ESR1/ER Alpha-andrographolide protein, and c) ESR1/ER Alpha-6 gingerol protein. The left side shows 3D visualization, the right side shows the types of bonds formed between ligand-protein.

(shown in green) for both ESR1/ER Alpha and AR proteins, three compounds demonstrated particularly promising results. Andropanolide exhibited strong binding potential with both ESR1 and AR, while 6-Gingerol showed high affinity for ESR1, and Sarcostin displayed favourable binding with AR. Notably, these compounds achieved binding energies at or below the significant -7 kcal/mol threshold, suggesting their ability to form efficient, rapid, and stable bonds.

Interactions were formed between the target protein and each of the top 2 ligands as well as the native ligand. Based on the types of bonds produced, hydrophobic bonds and van der Waals bonds were the most dominant. Residues in bold font are amino acid residues from the PDB control ligand that are maintained in samples with the same bond type. Meanwhile, residues in italic font are those maintained in samples but with altered bond types and distances. Based on the analysis of active sites, amino acid residues, high affinity, and low binding energy are supported by the ability to maintain key amino acids, ensuring activity similar to that of the native ligand control. Figs. 7 and 8 shows the 3D visualisation results of the target protein complex with the sample and control ligands.

Research supports the finding that the compound 24-Methylcholesta-7,22-dien-3β-ol, a natural sterol, interacts with estrogen receptors through its steroid structure. This compound demonstrates moderate affinity for estrogen receptors and acts as a weak partial agonist. Sarcostin shows a similar interaction pattern but with its own unique characteristics, interacting with estrogen receptors via a more selective mechanism and affecting estrogen signalling pathways more

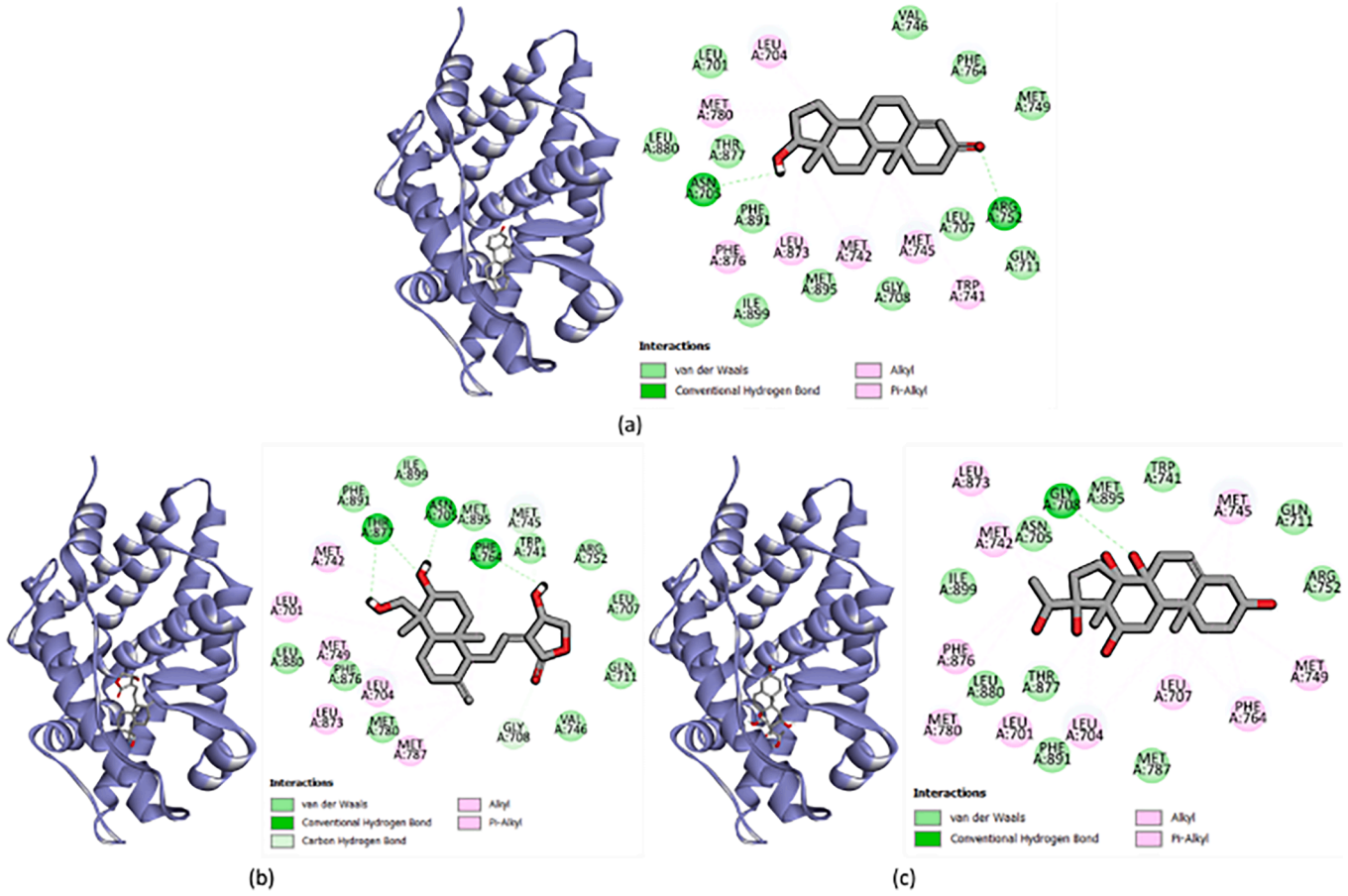

Fig. 8. Docking results visualization, a) AR-testosterone protein (pdb control), b) AR-andropanolide protein, and c) AR-sarcostin protein. The left side shows 3D visualization, the right side shows the types of bonds formed between ligand-protein.

specifically. Recent research has shown that steroid hormone regulation through ESR1/ESR2 and AR is crucial for follicle maturation and spermatogenesis [35]. Smolarz et al., found that CYP17A1 and CYP19A1 play important roles in fertility therapy by regulating steroid hormone balance, affecting oocyte quality, and supporting embryo implantation [36].

The simulation study examined four samples: ESR1 (Estrogen receptor alpha/ERα) as a single target, and three complexes – ESR1_ETD (ESR1/Estradiol), ESR1_6GR (ESR1/6-Gingerol), and ESR1_ADP (ESR1/Andropanolide). The potential energy analysis of single and complex structures revealed significant changes during the simulation. All four samples showed a marked increase in average potential energy from 0 ns to 0.025 ns (Fig. 9), indicating initial energy stabilization processes. Fluctuations continued even after reaching the equilibrium phase, with increases suggesting strengthened molecular bonds and decreases indicating molecular bond relaxation. The different equilibrium values between single ESR1 and its complexes with ligands demonstrated that ligand docking affects potential energy, which is one consequence of ER alpha protein activation.

The MMPBSA calculation combined gas-phase energy, free solvation energy, and solute entropy configuration contributions. MMPBSA analysis of the three complexes showed similar average free energy values against the implicit solvent during the 10 ns simulation, ranging from -2.0938 to -3.5758 kJ/mol. The control sample ESR1_ETD exhibited the highest MMPBSA value among all compounds (Fig. 10), while ESR1_6GR showed a higher value compared to ESR1_ADP.. This supports the potential of active compounds such as 6-Gingerol (6GR) to regulate hormone pathways through the estrogen receptor ESR1, enhance mitochondrial stability, and reduce oxidative stress. Therefore, it can be concluded that these active compounds have the potential to improve oocyte quality and support infertility therapy through hormonal regulation and cellular protection mechanisms.

YASARA analysis revealed three distinct types of hydrogen bond measurements: solute hydrogen bonds (Fig. 11a), solute-solvent hydrogen bonds (Fig. 11b), and ligand binding energy (Fig. 12). The results showed that when the test compounds 6GR and ADP formed complexes with ESR1, they exhibited fewer solute hydrogen bonds compared to ESR1 alone. In contrast, the control complex ESR1_ETD demonstrated higher solute hydrogen bond formation than the other tested samples. Within cell buffer environments, this pattern reversed, with the ESR1_ADP complex showing the highest values. A reciprocal relationship exists between solute hydrogen bonds and solute-solvent hydrogen bonds over time. For all three complexes, the average hydrogen bond energy measurements ranged from 6 to 25 kJ/mol. Samples with higher solute-solvent hydrogen bond counts tend to display increased hydrophilic properties, and greater protein-solvent interactions correlate with enhanced solvent accessibility. The binding energy assessment revealed that the ESR1_ADP complex established the strongest ligand-protein interaction, forming five hydrogen bonds, while ESR1_6GR formed four bonds—one more than the ESR1_ETD control complex. A higher number of hydrogen bonds between ligand and protein typically enhances affinity and reduces binding energy [37].

SASA (Solvent Accessible Surface Area) represents the surface area of a protein that is exposed and available for interaction with surrounding solvent molecules. This measurement provides valuable insights into conformational changes, protein-ligand interactions, and protein-protein interactions. SASA is a key factor in understanding protein stability and folding/unfolding processes, and it is determined by

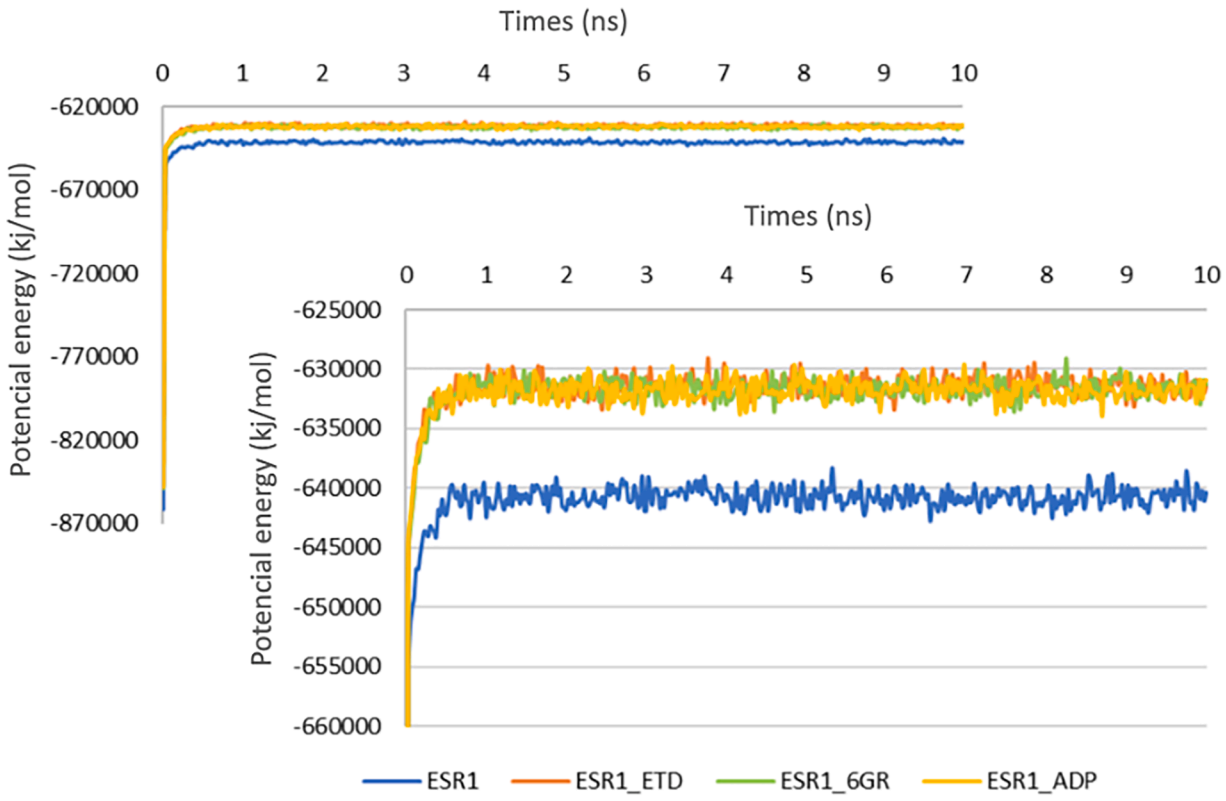

Fig. 9. Potential energy of single and complex proteins. Potential energy of single and ESR1 complex proteins shows the change in potential energy (kJ/mol) over simulation time in two graphs: the upper graph illustrates a larger potential energy scale to compare the complexes, while the lower graph zooms in to observe the potential energy fluctuations between single ESR1 (Blue), ESR1_ETD (Orange), ESR1_6GR (Green), and ESR1_ADP (Yellow).

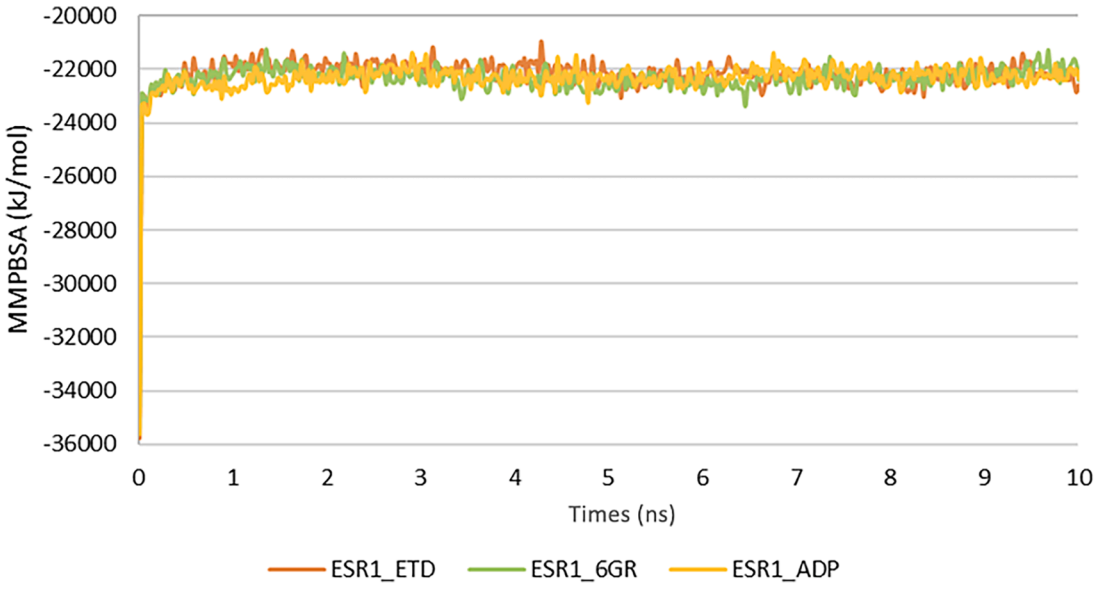

Fig. 10. Binding free energy (MMPBSA) profiles of ESR1 complexes (ESR1_ETD, ESR1_6GR, ESR1_ADP) during a 10 ns simulation. Lower MMPBSA values (more negative) indicate stronger binding stability. ESR1_ETD shows the highest stability, followed by ESR1_6GR and ESR1_ADP.

measuring the area accessible to a hypothetical solvent sphere in van der Waals contact with the molecular surface [38]. Higher SASA values typically indicate that a protein structure has expanded. When analysing activator compounds, expected to observe low SASA value fluctuations during simulation, as this suggests that the complex remains stable without significant conformational changes [39]. Our analysis revealed that, among all tested complexes, only ESR1_6GR showed an average SASA value lower than control ESR1_ETD. Furthermore, ESR1_ADP displayed the highest average SASA value, which aligned with its hydrogen bonding patterns, as illustrated in Fig. 13.

In Fig. 14, all four samples show an increasing RMSD trend with fluctuations. ESR1_ADP is the only sample that peaks above 3 Å, though its average remains below 2.5 Å. These results align with the H-bond and SASA analyses, indicating minimal structural changes in both the test

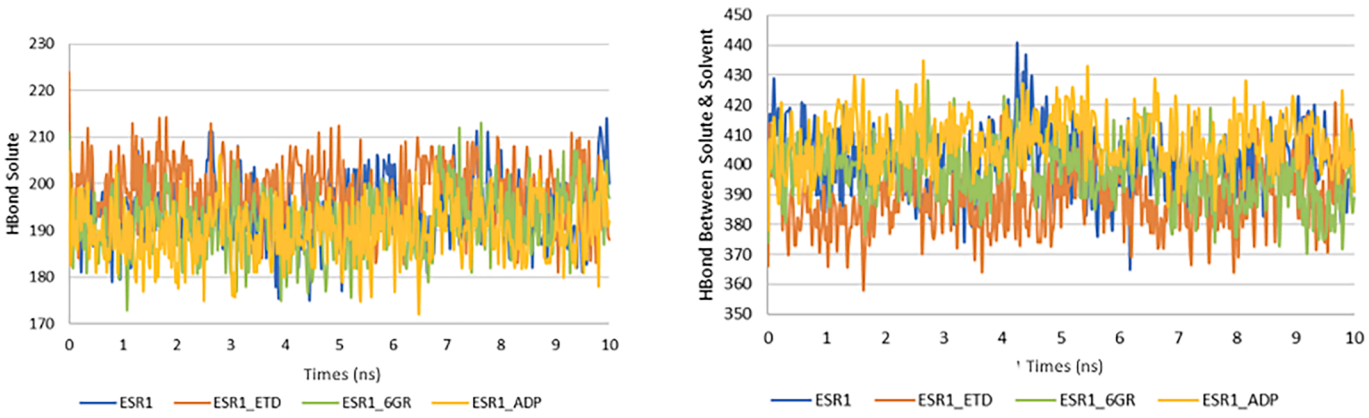

Fig. 11. (a): Stability of the Protein-Ligand Complex. The number of internal hydrogen bonds within the ESR1 protein complex and its ligands ETD, 6GR, ADP, indicating the stability of interactions in the binding pocket. **(b): Role of the Solvent.** The number of hydrogen bonds between the ESR1-ligand complex and the solvent, illustrating the ligand's adaptation to the aqueous environment for its biological function.

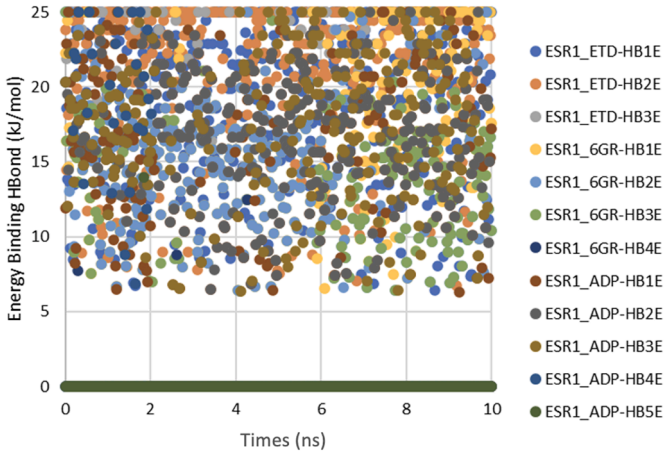

Fig. 12. Analysis of hydrogen bond energy between the protein complex and its ligand.

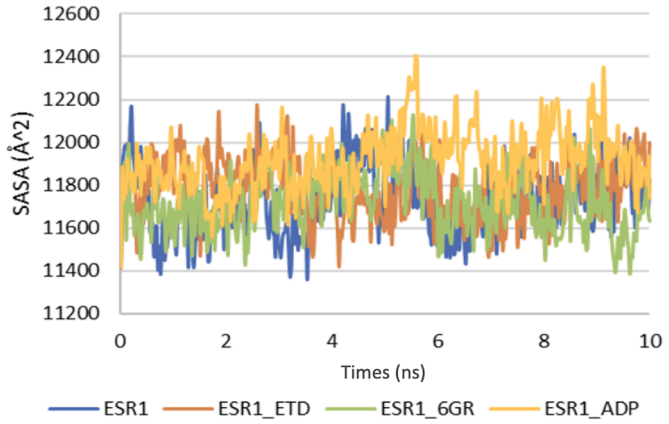

Fig. 13. Solvent Accessible Surface Area (SASA) measurements for individual molecules and molecular complexes.

compounds and the control.

Fig. 15 shows that C-alpha and Backbone RMSD data indicate all complexes have higher average values than single ESR1. In the 10 ns ligand movement analysis (Fig. 9a), only the ETD control ligand maintains an RMSD below 2 Å, while configuration analysis (Fig. 9b) shows

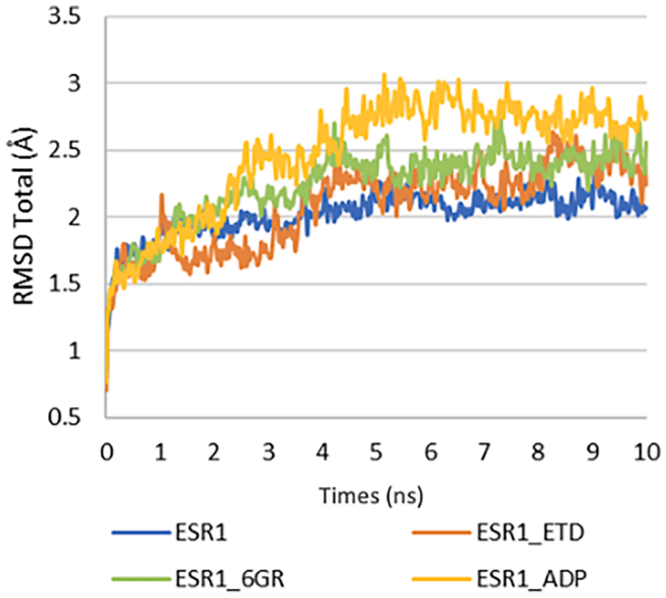

Fig. 14. Total RMSD values for individual molecules and complexes.

that only 6GR averages above 2 Å. This suggests that sea cucumber compounds have lower binding stability compared to the ETD control, with both test compounds showing significant position shifts while seeking better binding positions. However, ADP exhibits better configuration stability compared to 6GR.

The analysis showed that the control ligand ETD did not alter the original RG pattern of the ESR1 protein. In contrast, sea cucumber compounds caused notable changes in the ESR1 RG pattern, showing a gradual decrease that indicates the protein adopted a more compact, folded structure. The ESR1_ADP simulation displayed an initial peak, suggesting the protein briefly existed in an unfolded state at the start of the process. These findings are visually confirmed through structural comparisons before and after the simulation, as shown in Fig. 16.

The superimposition analysis of the four samples before and after simulation provides detailed insights into how ligand binding affects ESR1 protein conformational stability, as shown in Fig. 17. The visualisation clearly demonstrates configuration changes for each ligand. These superimposition results align with the H-bond, SASA, and RMSD analyses, confirming that both the control ligand and test compounds maintain the overall ER alpha protein conformation. Notably, the test compounds' ligands exhibit significant changes in their binding

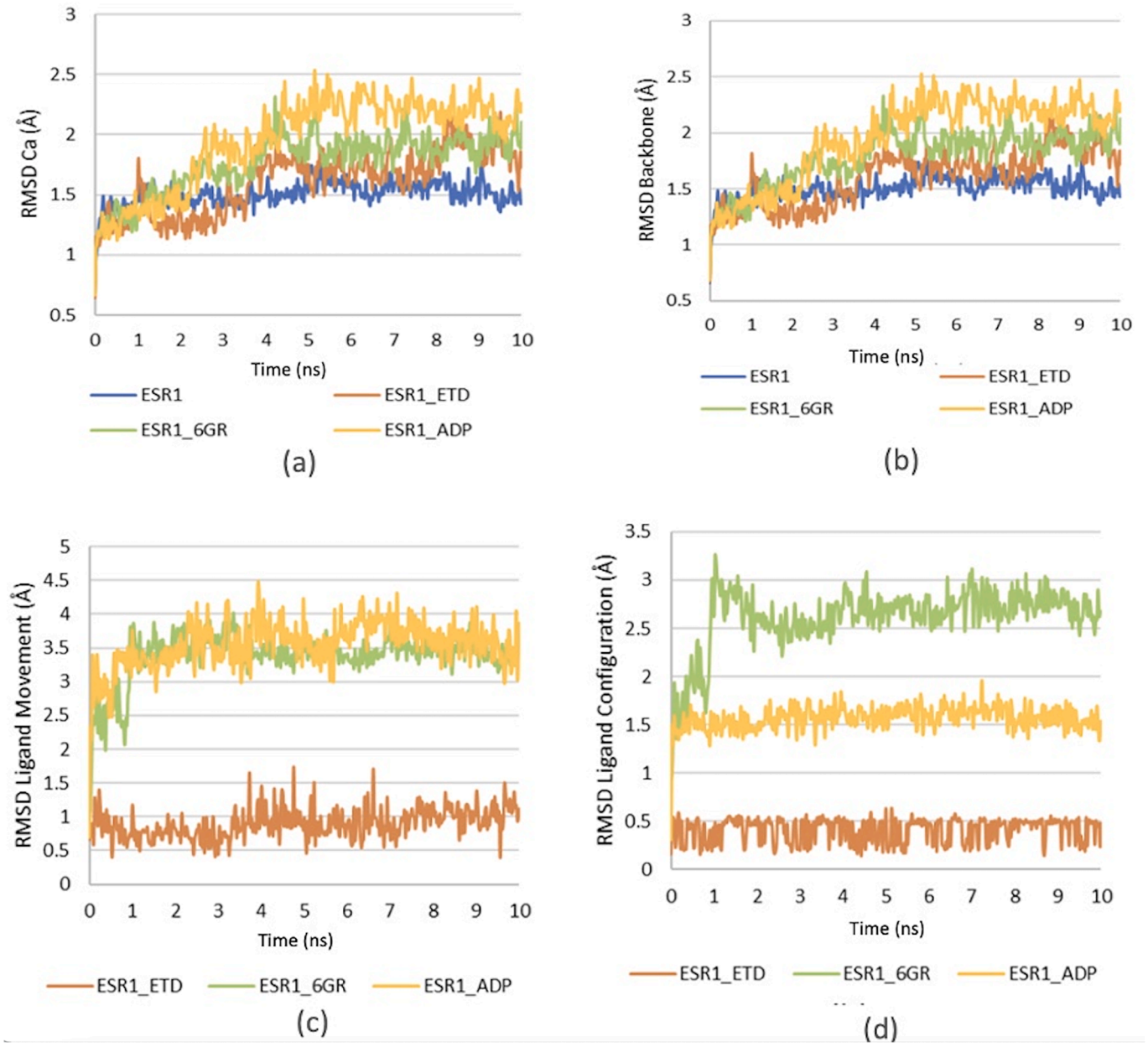

Fig. 15. Analysis of protein-ligand dynamics: (a) RMSD Cα; (b) RMSD backbone; (c) Ligand movement (d) Ligand configuration.

positions and structural configurations.

Root Mean Square Fluctuation (RMSF) analysis helps evaluate structural changes by measuring how individual amino acid residues and ligand nucleotides move within a protein. In our study of the ESR1 protein structure, RMSF measurements showed that some residues moved by more than 3 Å, both in the isolated protein and when bound to ligands, as illustrated in Fig. 18. Importantly, no residues showed movements exceeding 5 Å, suggesting that while the bonds experienced relaxation, they remained stable and did not break.

The *in silico* analysis of Stichopus herrmanni extracts revealed that their bioactive compounds have the potential to influence hormonal pathways important for fertility. Among these compounds, andrographolide, 6-gingerol, and sarcostin showed the strongest interactions with key hormone receptors. The ESR_6-gingerol complex demonstrated better affinity and binding stability than ESR_andrographolide at 20 ns. Because of their superior stability at this time point, only the ESR_6-gingerol complex and ESR_Estradiol as a control were evaluated at 100 ns. The extended simulation confirmed improved stability and binding, as indicated by better RMSD, RMSF, SASA, and MMPBSA values.

Fig. 19 shows molecular dynamics simulations of the ESR1 receptor in complex with ETD and 6-gingerol over 100 ns. Both ligands maintained the structural stability of ESR1, as indicated by low average RMSD values: 0.15 nm for ETD and 0.19 nm for 6-gingerol. No significant conformational changes were observed. The average RMSF values were also low for both complexes—0.08 nm for ETD and 0.11 nm for 6-gingerol—indicating minimal increases in residue flexibility and no signs of protein unfolding. Although the solvent-accessible surface area (SASA) was slightly higher with 6-gingerol at 131.27 nm^2 compared to 127.56 nm^2 for ETD, this small increase did not affect protein stability. The Molecular Mechanics Poisson-Boltzmann Surface Area (MMPBSA) analysis showed that 6-gingerol had a more favorable binding free energy (ΔTOTAL at -31.29 kJ/mol) compared to ETD (ΔTOTAL at -24.81 kJ/mol), suggesting better binding affinity and greater complex stability for 6-gingerol [40]. Overall, these results indicate that both ETD and 6-gingerol are compatible with ESR1, preserving its structural integrity

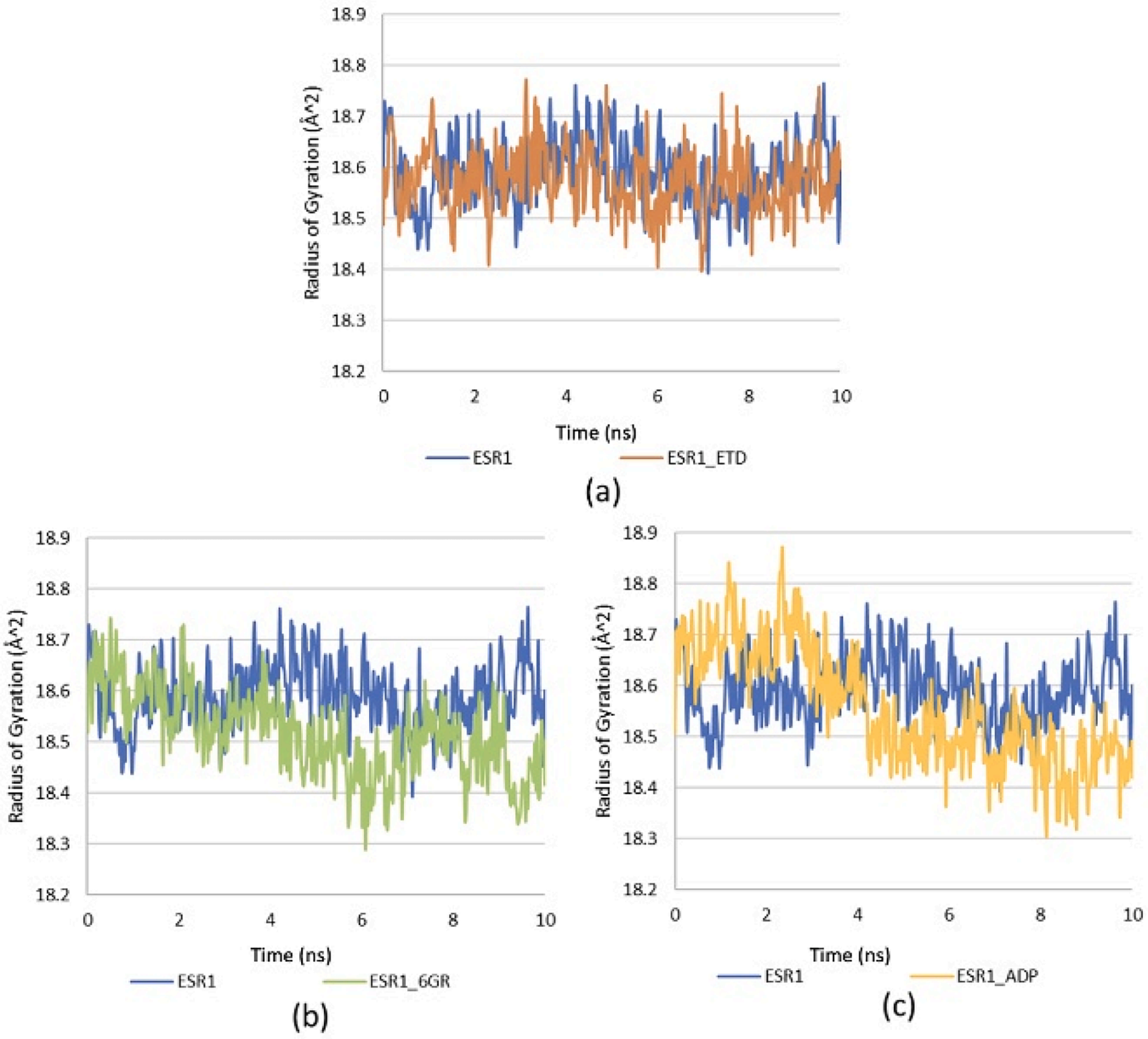

Fig. 16. Comparative analysis of RG patterns: single ESR1 protein versus complexes (a) ESR1_ETD, (b) ESR1_6GR, and (c) ESR1_ADP.

and dynamic stability throughout the simulation, with 6-gingerol showing a higher affinity and potentially more stable interaction than ETD. Although 6-gingerol can maintain the conformational stability of ESR1, its effect is slightly lower compared to the control, ETD. This appears to be due to the stronger binding affinity and stability of 6-gingerol compared to the native ligand, ETD.

Otherside, the modulation of estrogen and androgen signaling via ESR1, ESR2, and AR is another mechanism through which these bioactive compounds restore hormonal balance and improve reproductive health. In particular, the protein network pathway exhibits strong antioxidative properties by the Nrf2 pathway. This will improve oocyte quality. The dual therapeutic effects of these compounds not only emphasize their potential for treating infertility but also suggest their promise in managing menopausal symptoms.

In vivo results

Biochemical results

The data in the table shows that administering extracts can help improve the biochemical effects of a high-fat diet. This includes reducing triglycerides, glucose levels, triglyceride index, and weight gain. The use of extracts in the HFD group demonstrated the most effective results in improving these parameters.

Table 3 shows a significant reduction in the body weight of rats before and after treatment. NF-κB levels increased significantly with the administration of a high-fat diet (HFD), but this increase was significantly reduced by the extract. The highest average GSH levels were observed in the normal diet group, followed by the HFD with extract group, and the lowest in the HFD without extract group.

The bioactive compounds from sea cucumber show great potential in treating age-related infertility, as demonstrated by *in vivo* and *in silico* studies. These compounds exert antioxidant effects via the NFE2L2

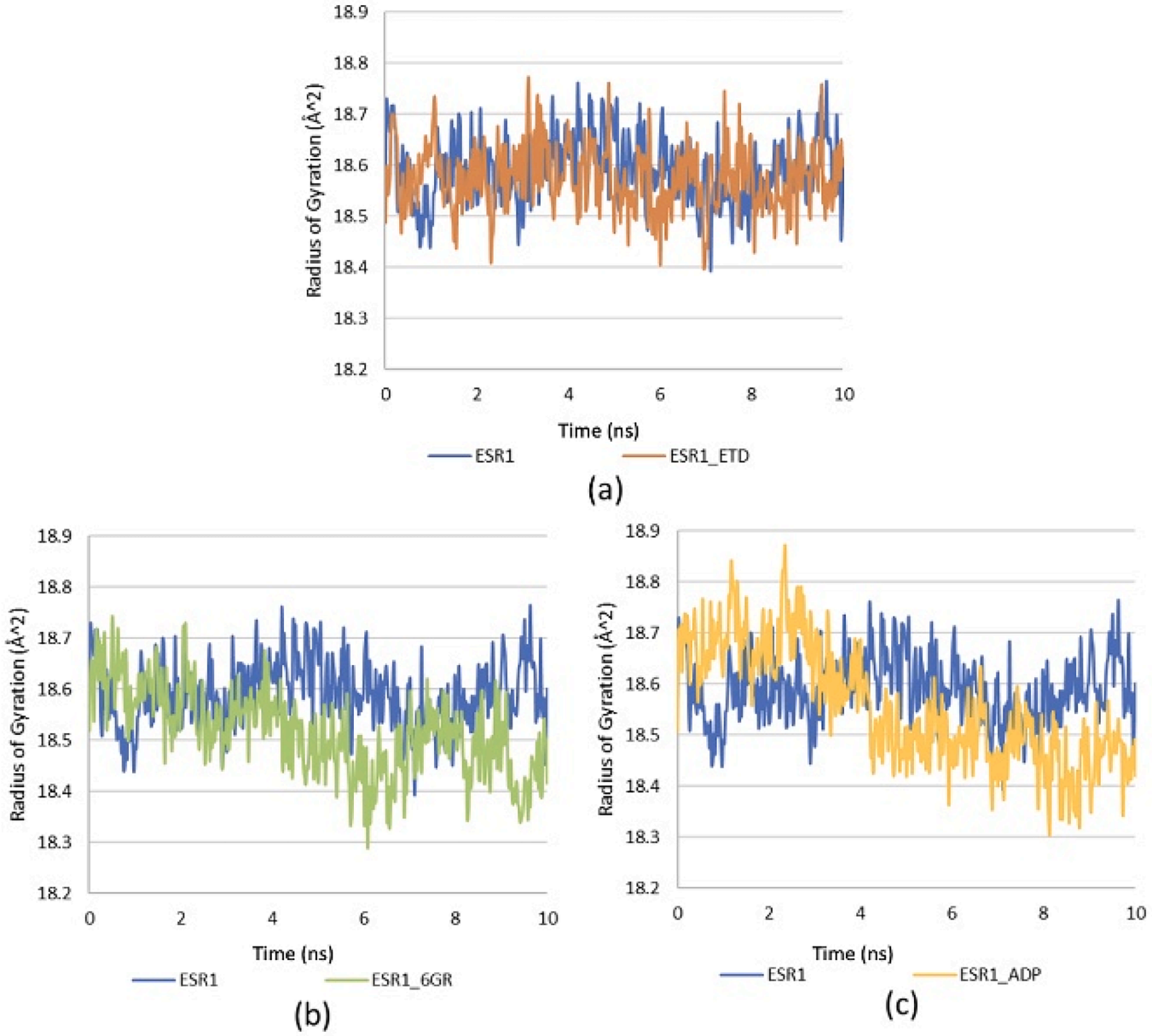

Fig. 17. Superimposition of ESR1 protein structures before and after molecular dynamics simulation. The initial conformations (green/orange) and final conformations (purple/pink) are shown for (a) ESR1 wild type, (b) ESR1 complexed with etoposide (ESR1_ETD), (c) ESR1 complexed with 6-gingerol (ESR1_6GR), and (d) ESR1 complexed with andrographolide (ESR1_ADP).

(Nrf2) pathway, reducing mitochondrial oxidative stress by activating enzymes like superoxide dismutase (SOD), catalase, and glutathione peroxidase (GPx). They protect reproductive tissues and support cellular health, with mitochondrial proteins like MT-ND1 and NDUFA further enhancing redox balance.

Anti-inflammatory effects are mediated through the MAPK3 (ERK1) pathway, which reduces pro-inflammatory mediators like NF-κB and supports tissue regeneration. The estrogen signaling pathway involving ESR1, ESR2, and AR restores hormonal balance, improving reproductive functions. Recent studies have shown that Erβ can suppress NF-κB activity [41]. Molecular docking studies confirm the ability of these compounds to influence these pathways. Thompson's study highlighted the fertility benefits of compounds like stigmasterol, which improved endometrial receptivity, 6-gingerol, which enhanced sperm quality, and platycodigenin, which supported follicle development [42]. Another study by Wang, found that adding these compounds to ovarian stimulation protocols increased IVF success rates by 23% [1]. By promoting ovulation, folliculogenesis, and endometrial receptivity, these compounds provide a promising, personalized approach to combat infertility and improve reproductive health [43].

Conclusion

Through *in silico* study, key bioactive compounds such as andrographolide, 6-gingerol, and sarcostin were identified as effectively interacting with hormone receptors. These compounds play a critical role in hormonal regulation. Additionally, *in vivo* studies demonstrated their antioxidant properties, which help reduce oxidative stress. The dual action of these compounds show the potential of *Stichopus herrmanni* extract as a promising therapy for infertility, particularly age-related infertility.

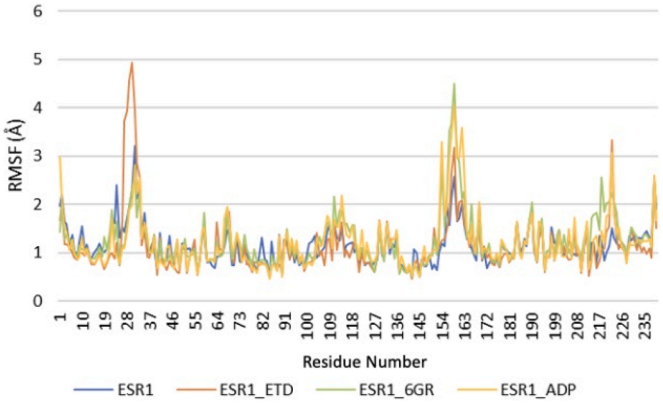

Fig. 18. Root mean square fluctuation (RMSF) analysis of ESR1 protein residues, both unbound and when bound to etoposide, 6-gingerol, and andrographolide.

Funding

This study was financially supported by the Research Institute of Universitas Muhammadiyah Prof. Dr. Hamka under contract number 594/F.03.07/2023.

CRediT authorship contribution statement

Irena Ujianti: Writing – original draft, Methodology, Funding acquisition, Formal analysis, Conceptualization. **Mulyoto Pangestu:** Supervision, Methodology, Investigation, Conceptualization. **Supandi:** Software, Methodology. **Bety Semara Lakhsmi:** Software, Methodology. **Wawang S Sukarya:** Software, Methodology. **Zahra Nurusshofa:** Project administration. **Takashi Yashiro:** Supervision.

Table 3
Effect of sea cucumber extract in biochemical parameters.

Parameter (Aorta Homogenat)	Normal Diet	High Fat Diet (HFD)	HFD + Extract
NfkB (ng/ml)	0.06 ± 0.01	0.36 ± 0.06	0.14 ± 0.02**
GSH (mg/dl)	478.3 ± 49.0	373.8 ± 31.8	221.9 ± 79.7**
Weight difference (before- after treatment)	23.8 ± 3.02	60.20 ± 10.6	24.8 ± 4.86**

The effect of sea cucumber extract on animal and biochemical parameters. The data is presented as mean ± SD values (n = 5 per group). The statistical differences were revealed by one-way ANOVA and Tukey's post hoc test. The mean differences were significant compared with the High Fat Diet group ($P < 0.05$, **$P < 0.01$, ***$P < 0.001$).

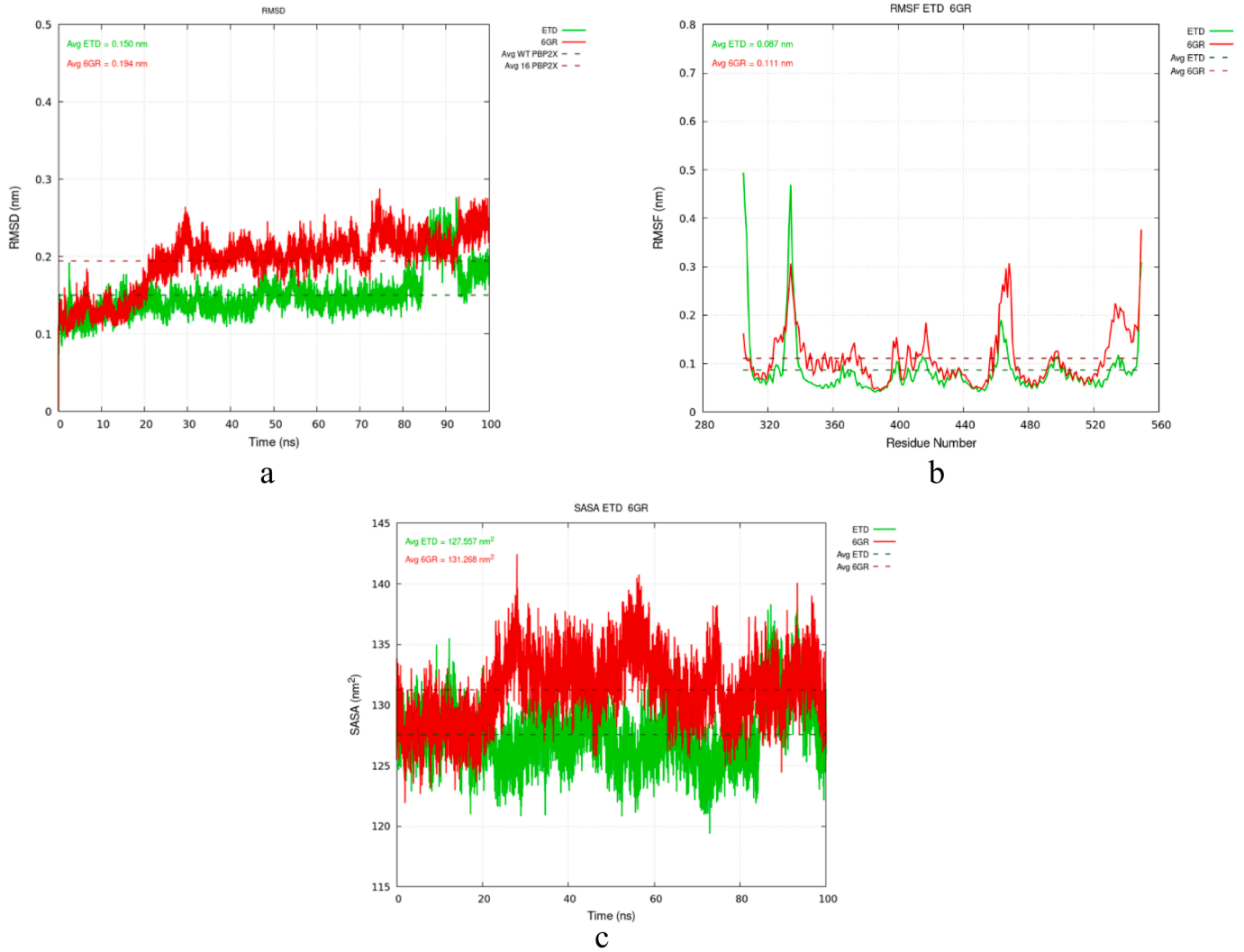

Fig. 19. Compability between ESR1_ETD (green) and ESR1_6 gingerol (red) over 100ns (a) RMSD plot comparing the structural stability (b) The RMSF plot shows the flexibility of amino acid residues (c) The SASA plot presents the solvent-accessible surface area.

Declaration of competing interest

The authors declare no competing interests.

Acknowledgements

We extend our heartfelt gratitude to the Faculty of Medicine at Universitas Muhammadiyah Prof. Dr. Hamka for their generous support, which made this research possible. We would also like to acknowledge and express our appreciation to all individuals who have provided assistance throughout this research process.

Data availability

No data was used for the research described in the article.

References

[1] Wang X, Zhang Y, Li H. Integration of bioactive compounds with conventional ovarian stimulation protocols improves IVF outcomes: a prospective clinical study. J Assist Reprod Genet 2024;41(1):145–58. https://doi.org/10.1007/s10815-023-02874-2.
[2] Brannigan RE, Hermanson L, Kaczmarek J, Kim SK, Kirkby E, Tanrikut C. Updates to male infertility: AUA/ASRM guideline (2024). J Urol 2024:10–1097.
[3] Carson SA, Kallen AN. Diagnosis and management of infertility: a review. JAMA 2021;326(1):65–76.
[4] Ding H, Zhang J, Zhang F, Zhang S, Chen X, Liang W, Xie Q. Resistance to insulin and elevated levels of androgen: a major cause of polycystic ovary syndrome. Front Endocrinol 2021;12:741764.
[5] Bonavina G, Taylor HS. Endometriosis-associated infertility: from pathophysiology to tailored treatment. Front Endocrinol 2022;13:1020827.
[6] Xiao C, Wang J, Zhang C. Synthesis, regulatory factors, and signaling pathways of estrogen in the ovary. Reprod Sci 2023;30(2):350–60.
[7] Ujianti I, Semara Lakshmi B, Nurusshofa Z, Sukarya W, Indriyanti L. Network pharmacology analysis reveals bioactive compounds and potential targets of sea cucumber for cervical cancer therapy. F1000Res 2023;12:1358.
[8] Ujianti I, Lakhsmi BS, Nurusshofa Z, Sukarya WS. Evaluation of the potential of *Stichopus herrmanni* extract in inhibiting cervical cancer cell proliferation. Phytomed Plus 2024;4(3):100577.
[9] Hossain A, Dave D, Shahidi F. Antioxidant potential of sea cucumbers and their beneficial effects on human health. Mar Drugs 2022;20(8):521.
[10] Hoang TH, Liang Q, Luo X, Tang Y, Qin JG, Zhang W. Bioactives from marine animals: potential benefits for human reproductive health. Front Mar Sci 2022;9:872775.
[11] Luo X, Liu W, Zhao M, Wang J, Gao X, Feng F. The evaluation of sea cucumber (Acaudina leucoprocta) peptide on sex hormone regulation in normal and premature ovarian failure female mice. Food Funct 2023;14(3):1430–45.
[12] Kowalczyk A, Gałęska E, Szul A, Łącka K, Bubel A, Araujo JP, Wrzecińska M. Fertility rate and assessment of the cytoprotective capacity of various types of Holothuroidea extracts on spermatozoa. Vet Sci 2022;9(4):189.
[13] Moghadam FD, Baharara J, Balanezhad SZ, Jalali M, Amini E. Effect of *Holothuria leucospilota* extracted saponin on maturation of mice oocytes and granulosa cells. Res Pharm Sci 2016;11(2):130–7.
[14] Dong J, Wang NN, Yao ZJ, Zhang L, Cheng Y, Ouyang D, Lu AP, Cao DS. ADMETlab: a platform for systematic ADMET evaluation based on a comprehensively collected ADMET database. J Cheminform 2018;10:1.
[15] Xiong G, Wu Z, Yi J, Fu L, Yang Z, Hsieh C, Yin M, Zeng X, Wu C, Lu A, Chen X. ADMETlab 2.0: an integrated online platform for accurate and comprehensive predictions of ADMET properties. Nucleic Acids Res 2021;49(W1):W5–14.
[16] Daina A, Michielin O, Zoete V. SwissTargetPrediction: updated data and new features for efficient prediction of protein targets of small molecules. Nucleic Acids Res 2019;47(W1):W357–64.
[17] Keiser MJ, Roth BL, Armbruster BN, Ernsberger P, Irwin JJ, Shoichet BK. Relating protein pharmacology by ligand chemistry. Nat Biotechnol 2007;25(2):197–206.
[18] Ochoa D, Hercules A, Carmona M, Suveges D, Gonzalez-Uriarte A, Malangone C, Miranda A, Fumis L, Carvalho-Silva D, Spitzer M, Baker J. Open targets platform: supporting systematic drug–target identification and prioritisation. Nucleic Acids Res 2021;49(D1):D1302–10.
[19] Piñero J, Ramírez-Anguita JM, Saüch-Pitarch J, Ronzano F, Centeno E, Sanz F, Furlong LI. The DisGeNET knowledge platform for disease genomics: 2019 update. Nucleic Acids Res 2020;48(D1):D845–55.
[20] Szklarczyk D, Kirsch R, Koutrouli M, Nastou K, Mehryary F, Hachilif R, Gable AL, Fang T, Doncheva NT, Pyysalo S, Bork P. The STRING database in 2023: protein–protein association networks and functional enrichment analyses for any sequenced genome of interest. Nucleic Acids Res 2023;51(D1):D638–46.
[21] Sherman BT, Hao M, Qiu J, Jiao X, Baseler MW, Lane HC, Imamichi T, Chang W. DAVID: a web server for functional enrichment analysis and functional annotation of gene lists (2021 update). Nucleic Acids Res 2022;50(W1):W216–21.
[22] Jakubec D, Skoda P, Krivak R, Novotny M, Hoksza D. PrankWeb 3: accelerated ligand-binding site predictions for experimental and modelled protein structures. Nucleic Acids Res 2022;50(W1):W593–7.
[23] Bell EW, Zhang Y. DockRMSD: an open-source tool for atom mapping and RMSD calculation of symmetric molecules through graph isomorphism. J Cheminform 2019;11:1–9.
[24] Abraham MJ, Murtola T, Schulz R, Páll S, Smith JC, Hess B, Lindah E. Gromacs: high performance molecular simulations through multi-level parallelism from laptops to supercomputers. SoftwareX 2015;1–2:19–25. https://doi.org/10.1016/j.softx.2015.06.001.
[25] Yoshikawa M, Morikawa T, Oominami H, Matsuda H. Absolute stereostructures of olibanumols A, B, C, H, I, and J from olibanum, gum-resin of *Boswellia carterii*, and inhibitors of nitric oxide production in lipopolysaccharide-activated mouse peritoneal macrophages. Chem Pharm Bull 2009;57(9):957–64.
[26] Bader GD, Hogue CW. An automated method for finding molecular complexes in large protein interaction networks. BMC Bioinform 2003;4:2.
[27] Benjamini Y, Hochberg Y. Controlling the false discovery rate: a practical and powerful approach to multiple testing. J R Stat Soc Ser B (Methodol) 1995;57(1):289–300.
[28] Chen MN, Lin CC, Liu CF. Efficacy of phytoestrogens for menopausal symptoms: a meta-analysis and systematic review. Climacteric 2015;18(2):260–9.
[29] Ahmed F, Kamble PG, Hetty S, Fanni G, Vranic M, Sarsenbayeva A, Kristófi R, Almby K, Svensson MK, Pereira MJ, Eriksson JW. Role of estrogen and its receptors in adipose tissue glucose metabolism in pre- and postmenopausal women. J Clin Endocrinol Metab 2022;107(5):e1879–89.
[30] Hu YC, Wang PH, Yeh S, Wang RS, Xie C, Xu Q, Zhou X, Chao HT, Tsai MY, Chang C. Subfertility and defective folliculogenesis in female mice lacking androgen receptor. Proc Natl Acad Sci 2004;101(31):11209–14.
[31] Fan HY, Liu Z, Shimada M, Sterneck E, Johnson PF, Hedrick SM, Richards JS. MAPK3/1 (ERK1/2) in ovarian granulosa cells are essential for female fertility. Science 2009;324(5929):938–41.
[32] Siddappa D, Beaulieu É, Gévry N, Roux PP, Bordignon V, Duggavathi R. Effect of the transient pharmacological inhibition of Mapk3/1 pathway on ovulation in mice. PLoS ONE 2015;10(3):e0119387.
[33] Wang J, Dai S, Guo Y, Xie W, Zhai Y. Biology of PXR: role in drug-hormone interactions. EXCLI J 2014;13:728.
[34] Heidarzadehpilehrood R, Pirhoushiaran M, Abdollahzadeh R, Binti Osman M, Sakinah M, Nordin N, Abdul Hamid H. A review on CYP11A1, CYP17A1, and CYP19A1 polymorphism studies: candidate susceptibility genes for polycystic ovary syndrome (PCOS) and infertility. Genes 2022;13(2):302.
[35] Rodriguez AM, Garcia-Velasco J, Martinez F. Steroid hormone regulation through ESR1/ESR2 and AR: implications for follicular maturation and spermatogenesis. Fertil Steril 2024;121(2):341–55. https://doi.org/10.1016/j.fertnstert.2023.11.008.
[36] Smolarz B, Szyłło K, Romanowicz H. The genetic background of endometriosis: can ESR2 and CYP19A1 genes be a potential risk factor for its development? Int J Mol Sci 2020;21(21):8235.
[37] Trott O, Olson AJ. AutoDock Vina: improving the speed and accuracy of docking with a new scoring function, efficient optimization, and multithreading. J Comput Chem 2010;31(2):455–61.
[38] Pal P, Chakraborty S, Jana B. Number of hydrogen bonds per unit solvent accessible surface area: a descriptor of functional states of proteins. J Phys Chem B 2022;126(51):10822–33.
[39] Bagewadi ZK, Khan TY, Gangadharappa B, Kamalapurkar A, Shamsudeen SM, Yaraguppi DA. Molecular dynamics and simulation analysis against superoxide dismutase (SOD) target of *Micrococcus luteus* with secondary metabolites from *Bacillus licheniformis* recognized by genome mining approach. Saudi J Biol Sci 2023;30(9):103753.
[40] Valdés-Tresanco MS, Valdés-Tresanco ME, Valiente PA, Moreno E. Gmx_MMPBSA: a new tool to perform end-state free energy calculations with GROMACS. J Chem Theory Comput 2021;17(10):6281–91. https://doi.org/10.1021/acs.jctc.1c00645.
[41] Mal R, Magner A, David J, Datta J, Vallabhaneni M, Kassem M, Manouchehri J, Willingham N, Stover D, Vandeusen J, Sardesai S, Williams N, Wesolowski R, Lustberg M, Ganju RK, Ramaswamy B, Cherian M. A Estrogen receptor beta (ERβ): a ligand activated tumor suppressor. Front Oncol 2020;10:587386.
[42] Thompson RW, Anderson KL, Smith BD. Bioactive compounds in fertility enhancement: a multicenter analysis of stigmasta, 6-gingerol, and platycodigenin effects. Reprod Sci 2023;30(12):3456–70. https://doi.org/10.1007/s43032-023-01094-4.
[43] Lee EB, Chakravarthi VP, Wolfe MW, Rumi MK. ERβ regulation of gonadotropin responses during folliculogenesis. Int J Mol Sci 2021;22(19):10348.